Red Supergiant Stars within the Local Group

Lee. R. Patrick

Doctor of Philosophy
The University of Edinburgh
March 2016

Chapter 1

Spectroscopy and the K-band Multi-Object Spectrograph

1.1 Opening Remarks

KMOS warrants an individual chapter in this thesis as all of the spectroscopic observations used in this thesis are from this instrument. This chapter initially describes the basic design of a spectrograph and outlines some of the more commonly used spectroscopic techniques in Section 1.2. I then move on to describe integral field spectroscopy, a more complex spectroscopic technique, in Section 1.3. I then go on to describe KMOS in Section 1.4 and the KMOS data reduction process in Section 1.5. Finally, I conclude the chapter in Section 1.6.

1.2 Introduction to Spectroscopic Techniques

Spectroscopy is the study of the dispersion of light into its constituents and has been at the forefront of astronomy for roughly the last 200 years. Sir Isaac Newton demonstrated the principles of spectroscopy (and coined the term "spectrum") using light from The Sun in his seminal "Opticks" work (Newton, 1704). By using the groove spacings on a diffraction grating, Thomas Young first quantified the wavelengths of different colours of light (Young, 1802). The simple set-up of a spectrograph, which has - more or less - been used since the early spectroscopic experiments, consists of five basic elements:
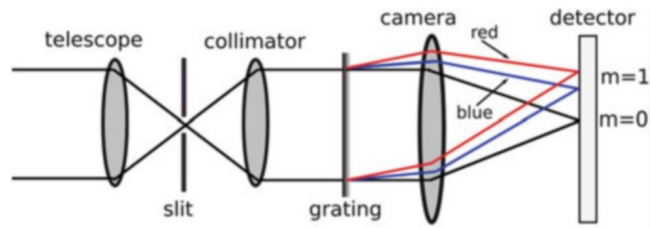
Figure 1.1 *A simple spectrograph detailing the five basic elements a spectrograph must posses: A slit, a collimator, a dispersive element, a camera and a detector. Credit: Lawrence (2014).*
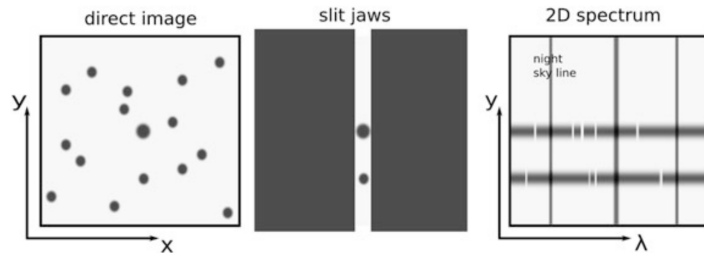
Figure 1.2 *Three panels demonstrating long-slit spectroscopy. The left panel shows what an image of the FoV would see. The central panel illustrates that the long slit selects only slit in the x-axis the full y-axis range. The right panel shows that for each pixel in the y direction, a spectrum is obtained. Credit: Lawrence (2014).*

   i Slit

  ii Collimator

 iii Dispersive element

 iv Camera

  v Detector

A simple spectrograph is illustrated in Figure 1.1. In Newton's demonstration he used a small hole in his window blinds as a slit and a screen as a detector. The slit in modern spectroscopic observations can take various forms. The most widely used type of slit, in modern observations, is long-slit spectroscopy. Using a long slit, a spectrum is taken for each spatial pixel along the length of the slit. This is demonstrated in Figure 1.3, where the final panel shows that each pixel illuminated by the slit produces a spectrum. This can be thought of a 2-dimensional spectroscopy, which is particularly useful when attempting to take a spectrum of an extended object (rather than a point source).

An alternative to using a long-slit to remove contamination from other sources is to use a small hole or fibre to select the target flux. By precisely drilling a hole in a metal plate, a slit is created which can be used to select the target flux. One of the advantages of using this method is that more than one object can be selected for a single exposure. By creating multiple slits within a single plate, spectroscopy of multiple objects can be obtained where contamination from other sources is minimised. An improvement to this method was to use optical-fibres positioned within the holes. The fibres could then be led to an instrument which was not directly attached to the telescope, which has the advantage that the instrument will not suffer from the changing gravitational force as the telescope moves. In addition, the conditions within the instrument room can be controlled. This is particularly important for near-IR spectrographs and detectors.

However, using a plate with several holes drilled into it has some drawbacks. These include the time in which it takes to create the slit mask, the lack of flexibility while observing and the operational costs of creating a new mask each time a different field is to be observed (Parry & Gray, 1986). These reasons, in addition to improved computing power, led to the development of instruments which were able to automatically position fibres (Tubbs, Goss & Cohen, 1982). Most modern fibre-fed spectrographs have automatic fibre-positioning technology which is broadly split up into two approaches.

i Each fibre has a magnetic button attached and a single robot is charged with moving each fibre sequentially. This is an effective method to place large numbers of fibres, but does however, take a significant length of time for each configuration.

ii Each fibre is mounted upon a computer-controlled arm. This method is generally less time consuming.

As a variant on the five basic elements of a spectrograph, slitless spectroscopy is also a feasible option which is not discussed in detail here. For a thorough overview on slitless spectroscopy see Cullen (????).

A key element to any spectrograph is the dispersive element. In Newton's original experiments this took the form of a glass triangular prism. A prism disperses light based on the wavelength dependence of the refractive index of glass: differential refraction. This produces a low-resolution spectrum spanning a large spectral range.
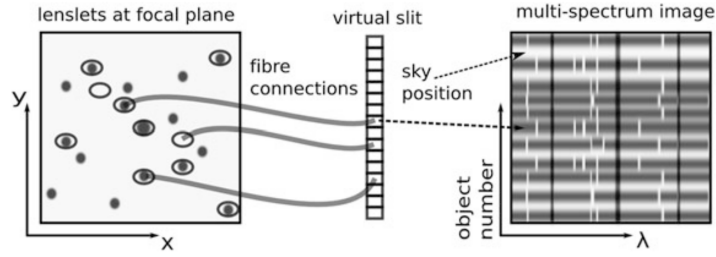
Figure 1.3 *Three panels demonstrating multi-object spectroscopy. The left panel shows what an image of the FoV would see. The central panel illustrates that each fibre in this simple multi-object spectrograph can be positioned at any point throughout the field of view and is rearranged into a pseudoslit. The right panel shows that for each pixel in the y direction, a spectrum is obtained. Credit: Lawrence (2014).*
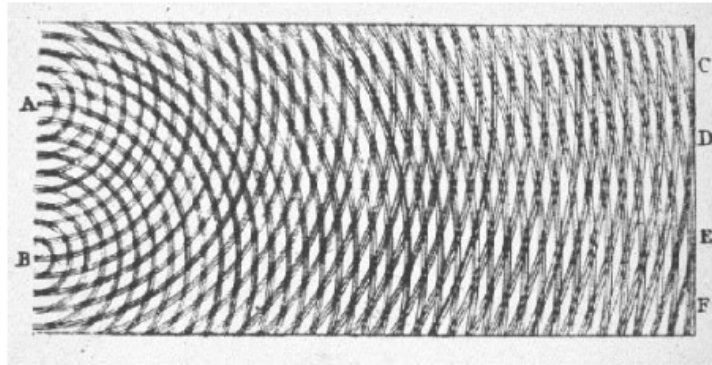
Figure 1.4 *A double slit interference pattern from Thomas Young's original experiments.*

Typically in modern spectrographs the dispersive element is a diffraction grating. A diffraction grating consists of a reflective surface with many parallel grooves. These grooves act as slits and disperse the light which is then combined on the detector through interference using the same principles as a double slit experiment. Figure 1.4 shows the interference pattern for monochromatic light striking two slits of width a with separation d at a wavelength λ. By increasing the number of slits the fringe maxima remain stationary while becoming narrower and more intense. The angular positions (θ) of the fringe maxima are,

$$sin\,\theta = \frac{m\lambda}{d},\tag{1.1}$$

where m is an integer and refers to the fringe order ($m = 0$ for the central undispersed peak). As the number of secondary peaks depends upon the number

of rulings N, the angular positions of the zero positions also depend upon N,

$$sin\,\theta = \frac{m'\lambda}{Nd}. \tag{1.2}$$

Therefore, the angular width of the principle maximum between the first two zero positions ($\Delta\theta$ or W) is obtained by defining,

$$W = \Delta m' \frac{d\theta}{dm'}, \tag{1.3}$$

and by differentiating equation 1.2,

$$W = \frac{2\lambda}{Nd\,cos\,\theta}. \tag{1.4}$$

The Rayleigh Criterion states: "Two point sources are regarded as just resolved when the principal diffraction maximum of one image coincides with the first minimum of the other" (Rayleigh, 1880). By the application of this criterion one can define the spectral resolution in terms of the angular separation as,

$$W = \frac{\lambda}{Nd\,cos\,\theta}. \tag{1.5}$$

which does not depend upon the fringe order. Typically, the spectral resolution is quoted in terms of the smallest wavelength which can be separated in the spectrum. This is given by converting the angular width into the corresponding wavelength width using $\Delta\lambda = \Delta\theta\,d\lambda/d\theta$ which gives,

$$\Delta\lambda = \frac{\lambda}{Nm}, \tag{1.6}$$

more commonly quoted as the ratio of the operating wavelength to the spectral resolution,

$$R = \frac{\lambda}{\Delta\lambda} = Nm, \tag{1.7}$$

where R is typically termed the spectral resolving power (or incorrectly as the resolution).

Separation of the spectral orders is an important consideration in diffraction grating spectroscopy which is usually taken into account using a broadband blocking filter to limit the spectral range to a single order only. In principle, higher spectral resolving power can be obtained by viewing higher spectral orders, however, the intensity of the spectra is diminished and the the spectral range is diminished. Typically low spectral orders are used in astrophysical observations.

Diffraction gratings have many intrinsic advantages over glass prisms when used for quantitative spectroscopy however they are used in tandem for some applications. Echelle spectrographs working in higher orders for larger resolving powers make use of an additional dispersive element, which is often a prism, to spatially separate different orders so that they can be simultaneously recorded on the detector.

Even though prisms are used rarely in modern astronomical spectroscopy they still have some important application. The upcoming James Webb Space Telescope (JWST) near infrared spectrograph NIRSpec will contain a prism (in addition to several diffraction gratings) to obtain low-resolution spectroscopy of a very large spectral range $(0.6–5.3\,\mu\mathrm{m})$.

1.3 Integral field spectroscopy

The overall goal with integral field spectroscopy (IFS) is to obtain a spectrum of everything (targets and their surroundings) within a given field of view (FoV). This concept builds on the idea that a long-slit spectrograph obtains spectra for targets within the extent of the slit. A natural extension of this technique would be to use a long-slit spectrograph to obtain a spectrum for each pixel within a 2-D FoV on the sky.

There are many intrinsic advantages to having a specifically designed instrument to perform this task rather than simply repeating observations with a long-slit spectrograph. These advantages include,

   i slit-losses are eliminated,

  ii accurate target acquisition is not required,

 iii the target position can be recovered from data,

iv reduced radial velocity errors from positional issues in the slit when comparing target and reference object,

v the velocity field is recovered without biases,

vi IFS always optimally samples object point spread function (PSF).

In addition, the potentially the most compelling argument is that to perform IFS with a long-slit spectrograph one is required to take N exposures all of length t_{exp}, however, using IFS, a spectrum for each spaxel is obtained with a single exposure. Therefore efficiency on-sky is increased.

1.3.1 Techniques of integral field spectroscopy

IFS may be achieved using a variety of different and novel methods. Potentially, the simplest of these is (and most cost effective in the short term) is to take multiple exposures using an existing spectrograph over a small FoV. Another, conceptually simple, approach is to take photometric data of the same field using multiple narrow-band filters which can be stitched together to create effectively low-resolution spectra of a FoV (e.g. GTC-OSIRIS Méndez-Abreu et al., 2011).

There are three main techniques which are more commonly used to generate spectra over a 2-dimensional FoV. An spectrograph specialised for integral fields adds an additional element to the five basic elements of a spectrograph outlined previously. This additional element is an integral field unit (IFU) which acts to split up the image obtained by the telescope into elements or slices which are constructed into a slit and dispersed by the dispersive element. The difference between the techniques is in the way in which they split up the image. In this section I will detail each of these techniques in turn and conclude by providing a comparison between the techniques.

A lenslet array splits the input image using a tight array of small lenses (Bacon et al., 1995). The lenses then focus the light of each sub-field separately which are then dispersed. This technique limits the length of the spectrum measured on the detector. To improve this the spectra are tilted about the optical axis to minimise overlapping of spectra, which leads to inefficient packing of the resulting spectra on the detector (e.g. Figure 1.3).

Fibre arrays use a tightly packed bundle of fibre-optic cables to split the telescope
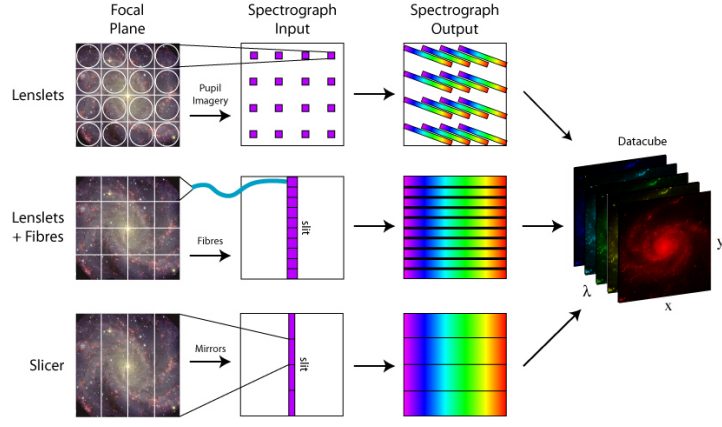
Figure 1.5 *Three diagrams demonstrating the techniques of IFS Credit: M. Westmoquette, adapted from (Allington-Smith, 2006).*

image (ref). The fibres are then reposition the image onto a linear slit. Figure 1.5 shows a cartoon of this process. As the fibre cables are intrinsically cylindrical objects, much light is lost between fibres. To minimise the light lost this technique can be improved upon by using an array of lenses to focus the light from each element into the fibre, effectively combining this technique with the previous method.

The final technique is to use an image slicer to split the image from the telescope (Content, 1997). Figure 1.6 shows an image slicer used in the KMOS instrument. An image slicer is a type of segmented mirror where each linear segment reflects light in a slightly different direction. A second segmented mirror then arranges the images into a pseudoslit where it is then dispersed. As Allington-Smith (2006) demonstrate, this method is intrinsically efficient as complete slices of the field are imaged by the detector. In addition, this method is also particularly applicable for IR studies as the optical system consists mainly of mirrors which are easily cooled to low temperatures. Drawbacks with this technique include that a large and complex optical system is required with a surface roughness (σ) of $\sigma \leq 10\,\mathrm{nm}$ in the IR.

Allington-Smith (2006) perform a detailed theoretical comparison between these three techniques and conclude that using an image slicer to split up the telescope image is the most efficient, by a considerable margin. Using fibres or lenslet arrays give similar performances, although lenslet arrays are easier to construct. Image slicer instruments, however, are the most complicated to construct owing to their complex optical systems.

Figure 1.6 *An image slicer from one of the arms used in the KMOS instrument. An image slicer is a type of segmented mirror which, in this case, slices the image into 14 different segments where each segment focuses the light in a slightly different direction. KMOS has 24 of these image slicers. Note: Image retrieved from the ESO website: https://www.eso.org/sci/facilities/develop/instruments/kmos.html*

1.4 The K-band Multi Object Spectrograph

KMOS is a second generation instrument on the Very Large Telescope (VLT), Chile which completed its design review in 2008 and completed commissioning in April 2013. As its name suggests, KMOS is a multi-object spectrograph operating at near-IR wavelengths (providing coverage from 0.8–2.5 μm), which hosts 24 IFUs. Therefore, KMOS can be described as a multi-object integral field spectrograph.

KMOS was designed specifically to provide spatially-resolved spectroscopy, while allowing multiple spectroscopic observations at near-IR wavelengths and was constructed by a consortium of UK and German institutes in collaboration with the European Southern Observatory (ESO). The final design of KMOS boasts 24 configurable arms, each hosting an IFU with a 2.8" × 2.8" FoV which can be placed at user-specified positions within a 7.2' FoV. These IFUs anamorphically magnify their individual sub-field onto one of the 24 advanced image slicers which partition each sub-field into 14 slices each with 14 spatial pixels. Therefore one KMOS IFU obtains 14×14 contiguous spectra in a single exposure.

The optical design of KMOS includes a three-fold symmetry about the Nasmyth optical-axis (see Figure 1.7. Each segment is designed to receive the light from
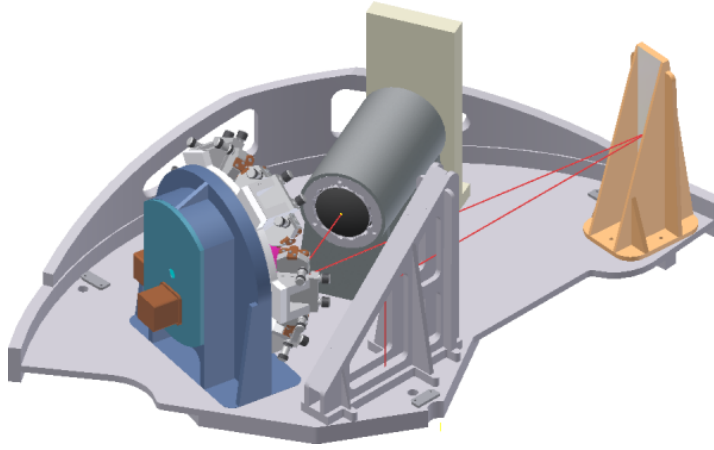
Figure 1.7 *The light path for a KMOS spectrograph demonstrated by the solid red line. The IFU entrance slit is located underneath the baseplate. The light path comes from the slit entrance and is redirected by the fold mirror toward the collimator (right, highlighted in yellow), where the light then is directed to the grating (left, housed in the blue filter wheel containing all 5 gratings) which disperses the light in camera barrel which finally focuses the light onto the detector (where the detector mount is in beige).*

8/24 of the configurable IFUs which is then passed to a cryogenic spectrograph containing five diffraction gratings (IZ, YJ, H, K and HK). Therefore, KMOS has three quasi-identical spectrographs which can be independently configured and set up.

KMOS was designed with specific science goals which revolved around the case for spatially resolving the structure in galaxies across a large range of redshifts and environments (Sharples et al., 2006) and, as the most-efficient near-IR multi-object spectrograph in the southern hemisphere, KMOS has gained significant attention from the wider community. Following successful commissioning runs KMOS underwent two science verification (SV) runs before being made available to the community for general observing in October 2013 (Sharples, 2015). Since then KMOS has been used to study many different science goals and has already had an impact in the fields of some of its key science drivers (Harrison et al., 2016; Magdis et al., 2016) as well as some intriguing results in other areas (Feldmeier-Krause et al., 2015; Parviainen et al., 2015)

In addition, KMOS has been exploited as a multi-object spectrograph to study the metallicities of star-forming galaxies using RSGs as cosmic abundance probes (Gazak et al., 2015; Lardo et al., 2015; Patrick et al., 2015). This programme is described in detail **??**. This thesis makes extensive use of KMOS
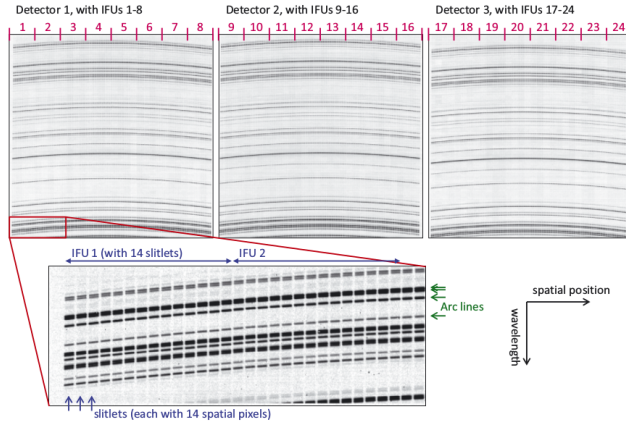
Figure 1.8 *A*
n example of a raw data product form KMOS taken from Davies, R. I. et al. (2013a). This figure illustrates that in one frame, light is dispersed onto one of three detectors. Each detector records light from eight IFUs which is dispersed roughly in alignment with the *y*-axis on the detector. Each IFU contains 14 spectra with a width of 14 detector pixels and therefore the *x*-axis roughly corresponds to the spatial axis.

and would not be possible without this state-of-the-art instrument.

1.5   Production of Three-dimensional Data Cubes

The nature of IFS is to obtain spatial and spectral information for each pixel on a detector. The final data product is, therefore, a three dimensional data cube consisting of two spatial and one spectral dimension. Therefore, the goal of the data reduction and calibration process is to create this regularly-sampled data cube from (often) several raw detector images.

As mentioned, the KMOS is arranged into three identical segments. Each segment contains eight IFUs which are arranged to project data onto a single detector. Each IFU contains an advanced image slicer which slices the field into 14 slices (see Figure 1.6) each of which contain 14 spatial pixels. Therefore, one IFU produces 196 individual spectra which means a single detector contains information on over 1500 spectra. An example of a raw data product with KMOS is illustrated in Figure 1.8 and highlights that each IFU contains 14 spectra each of width 14 pixels on the detector. This figure demonstrates how the dispersed spectra are arranged on the detector.

KMOS is designed so that on the detector, the y-axis roughly corresponds to the

spectral axis. However, on the detector there is no concept of spatial and spectral axes, only information which can be calibrated and reconstructed into a regularly sampled cube with spatial and spectral axes.

1.5.1 Calibration

To calibrate KMOS data each value recorded by the detector must be assigned spatial and spectral information. To do this one can use the projection of the light onto the detector, and the reliability of this projection, as a detailed diagnostic. Slitles are positioned on the detector to $\pm 1 \, \mu$m (roughly $1/18^{\text{th}}$ of a pixel; Davies, R. I. et al., 2013a) and the mean slit-width across the detector is 13.6 ± 0.1 pixels, where the error quoted here is the standard deviation of the mean from all slitlets. This pattern is so stable that subtle imprints of the opto-mechanical design of the instrument can be seen in the patterns (see Fig. 2 of Davies, R. I. et al., 2013a).

The main factor that affects this pattern is the temperature of the spectrograph. As with any IR instrument, the detector must be cryogenically cooled to minimise the effects of photons from the thermal background promoting electrons into the conduction band of the semi-conducting diode of the detector which are then confused with signal from the target. For KMOS the detectors are cooled to ≤ 80 K. In addition to the cooling of the detector, the optical bench – which houses the spectrographs – is also cooled to ≤ 140 K. However, the temperature of the optical bench is not controlled and can therefore vary with the ambient temperature of the surroundings by several Kelvin which has a small, but significant, effect on the positions of the slitlet edges when the positions of the slitlets are compared between calibration frames and science frames (described below). The implications of this potential temperature variation of the optical bench are that during calibration frames, the temperature must be within ± 1 K of the science frames.

To make use of the pattern of the slitlets on the detector to calibrate the raw data, two types of calibration frames are obtained. Flat lamp calibrations use a halogen lamp with a white-light spectral appearance to fully illuminate each slitlet and are used to calibrate the spatial positions of each detector pixel. Arc lamp calibrations use halogen lamps which create a spectrum containing several diagnostic spectral features which are used to calibrate the wavelength of each detector pixel. These calibration frames are then compared with the science
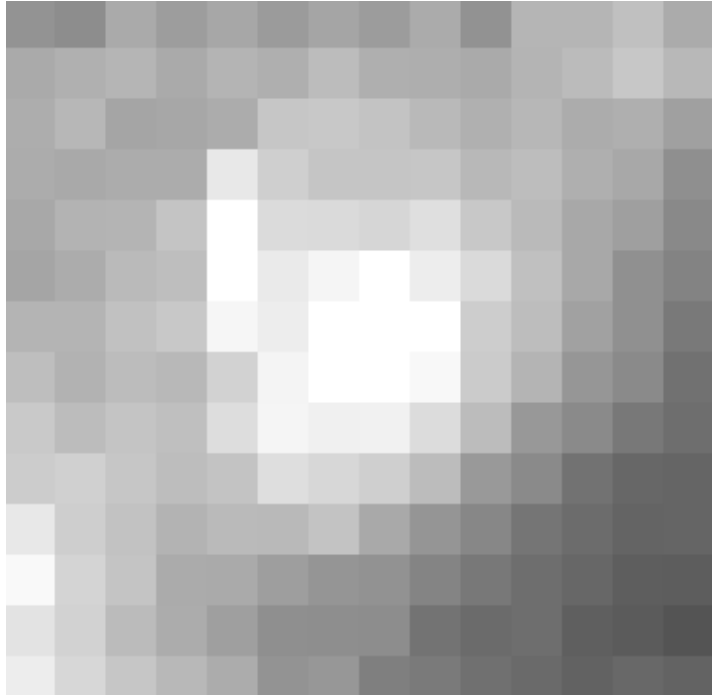
Figure 1.9 *An image of reconstructed KMOS IFU demonstrating, how each of the 14 slices of the field contains 14 pixels. This image is at a wavelength of 1.100 μm. A spectrum is produced for each pixel and the current image is a snapshot at one particular spectral pixel.*

frames to construct a three dimensional data cube for each IFU. An example of a reconstructed IFU is given in Figure 1.9. This figure is a snapshot of the reconstructed IFU at a particular wavelength.

Calibration of the KMOS data can be split into three distinct processes:

   i Flatfielding,

  ii Mapping data into a regularly-sampled cube,

 iii Correction for atmospheric and instrument transmission.

All of these processes are required to calibrate spectroscopic data in general, however, mapping the distortions of an instrument and transforming the data into a regularly sampled cube is necessarily an instrument-dependent approach and, because of the complexity involved in arranging eight IFUs onto a detector, is the most important set-up in calibrating KMOS data.

Flatfielding is the process which corrects for the difference in response from detector pixels and is performed in a standard fashion using halogen lamps.

Flatfielding is also used to correct for variations in the illumination of the KMOS IFUs. This is done directly using exposures from halogen lamps (lamp flats) and can be improved upon by using the twilight sky to illuminate the detector (sky flats). Using the twilight sky is generally (not just for KMOS but within spectroscopy in general) preferred as the light path is identical to that of the science exposures. However, observing in twilight conditions is extremely time dependent and in practice is difficult to undertake for an instrument as complex as KMOS.

To create the three dimensional data cube from KMOS raw data a look-up table is created containing information relating each detector value with spatial and spectral locations. This look-up table is implemented by creating three calibration files containing x, y and λ information for each pixel. These calibration frames are created by making use of the repeatability of the pattern of the slitlets on the detector. By fully illuminating the slitlets using the lamp-flat exposures the edge positions can be matched between the calibration and the science frames. This provides the two spatial coordinates for each detector value.

To calibrate the wavelength of the each detector pixel one must illuminate the detector with a spectrum where the wavelength of each spectral feature is precisely known (i.e. the arc flats). This is achieved with KMOS using a halogen lamp containing Neon and Argon where strong spectral features of known wavelengths cover the full detector range. By identifying a few isolated spectral lines within these exposures, which are then traced across the length of the detector, a polynomial function is used to assign each pixel with a wavelength value.

As KMOS is a roughly three tonne instrument, the effects of flexure can be significant and are mainly caused by rotation of the instrument on the Nasmyth platform. To account for this, calibration frames are taken at various rotator angles which are chosen to match the rotator angle of the science observations. Using calibration files at a more appropriate rotator angle can make a reasonable correction to the most serious sources of flexure.

At this stage, all the information needed to create the three dimensional data cube is available in three calibration files. This information is now used to transform the detector values onto a regularly sampled three dimensional data cube for each IFU. It is necessary to perform multiple interpolations to the detector values, rather than simply rearranging these values, as – in the frame of reference of the regularly sampled three dimensional data cube – the detector values are

irregularly sampled. This is obvious from Figure 1.8 which illustrates that the spectral and spatial axes are *roughly* aligned with the x and y axes of the detector respectively.

There are, in principle, many different methods to create the data cube which affect the spectral and spatial resolution of the final data product. The method which typically produces the highest quality data uses two (or three) one dimensional interpolations, the so-called "cubic spline interpolation" routine in the pipeline. This methods is makes use of two properties of the IFUs:

i each slitlet is a straight line when projected onto the sky,

ii the spacing across each slitlet is fixed and uniform (as a result of the properties of the image slicers).

By exploiting these properties this method is able to assign each detector pixel an x, y and λ value. This is achieved by – using ii – rearranging the detector values across each slitlet where no interpolation is necessary.[1]Subsequently a one dimensional cubic spline interpolation is performed along each slitlet, using i. A final one dimensional cubic spline interpolation is performed in the spectral direction. This method produces the best spectral resolution as well as giving highly consistent spatial resolution within each IFU.

The final step in calibrating KMOS data is to take into account the effects of the Earth's atmosphere. Observing from within the Earth's atmosphere affects the quality of the data in two different ways. Intrinsically, when observing an astrophysical source through the Earth's atmosphere, each illuminated detector pixel contains a combination of source and sky photons. Molecules and dust within the Earth's atmosphere scatter, absorb and emit light from the Earth and Moon which contaminates spectroscopic and photometric observations. To account for this one typically attempts to observe a sky spectrum without any signal from the astrophysical source. This usually takes the form of observing offset sky positions, where between each target exposure, sky targets are observed which are chosen to minimise contamination. This results in an additional set of sky frames which are then used to calibrate the science frames using the same IFU in both science and sky exposures. These sky frames are dealt with in the same manner as science frames in terms of calibration. Before the reconstruction

---

[1]This is the case when the default sampling is used, when any other sampling is requested this step requires an additional interpolation performed using the cubic spline method.

of the three-dimensional data cubes however, the sky frame which is nearest in time to the science frame in question is subtracted.

The second correction accounts for the absorption and re-emission of light from the science target by molecules within the Earth's atmosphere. As the sophistication of this step is highly dependent upon the science case of the observations, for the general user this is implemented in a simplistic manner. Typically, to perform this correction one observes an additional target of known spectral appearance: a telluric standard star. This star is observed in each of the 24 KMOS IFUs in turn (or three IFUs depending upon the quality of the correction required) and the frames are calibrated using the same process as the science observations.

A spectrum is extracted from each IFU which is then divided by a model of the transmission of the atmosphere, the stellar features are then modelled with a simple Lorentzian function and removed. This leaves a continuum spectrum of the star where the main features have been removed. At this point the transmission model is then multiplied back into the spectrum and the shape of the spectrum is corrected with a blackbody spectrum with the effective temperature of the star. Theoretically, these steps create a spectrum which contains only the light from the absorption of the Earth's atmosphere: the telluric spectrum. The final target spectrum from an individual IFU is then divided by the telluric spectrum.

1.6   Conclusions

In this chapter I have detailed the principles of spectroscopy and have outlined some of the key spectroscopic tools used to undertake astrophysical measurements, focussing on the diffraction grating and its uses in astronomy. I have described IFS in detail and outlined some of the innovations which make this novel method possible. I focus on using an advanced image slicer to perform IFS and outline why this method is superior to other approaches. This leads onto a description of the instrument which is used for the observations in this thesis: KMOS. In this section I detail some of the key features which make this instrument unique and highlight that KMOS has been applied to a range of science cases. Finally, I describe the data products from KMOS and detail the process of calibration of the raw data.

Bibliography

Allington-Smith J., 2006, New Astronomy Reviews, 50, 244

Bacon R. et al., 1995, A&AS, 113, 347

Content R., 1997, in Society of Photo-Optical Instrumentation Engineers (SPIE) Conference Series, Vol. 2871, Optical Telescopes of Today and Tomorrow, Ardeberg A. L., ed., pp. 1295–1305

Cullen F., ????, PhD thesis, Institute for Astronomy, University of Edinburgh

Davies, R. I. et al., 2013a, A&A, 558, A56

Feldmeier-Krause A. et al., 2015, A&A, 584, A2

Gazak J. Z. et al., 2015, ApJ, 805, 182

Harrison C. M. et al., 2016, MNRAS, 456, 1195

Lardo C., Davies B., Kudritzki R.-P., Gazak J. Z., Evans C. J., Patrick L. R., Bergemann M., Plez B., 2015, ApJ, 812, 160

Lawrence A., 2014, Astronomical Measurement: A Concise Guide

Magdis G. E. et al., 2016, MNRAS, 456, 4533

Méndez-Abreu J. et al., 2011, PASP, 123, 1107

Newton I., 1704, Opticks: or, a Treatise of the reflexions, refractions, inflexions and colours of light. Also two treatises of the species and magnitude of curvilinear figures. London

Parry I. R., Gray P. M., 1986, in Society of Photo-Optical Instrumentation Engineers (SPIE) Conference Series, Vol. 627, Instrumentation in astronomy VI, Crawford D. L., ed., pp. 118–124

Parviainen H., Aigrain S., Thatte N., Barstow J. K., Evans T. M., Gibson N., 2015, MNRAS, 453, 3875

Patrick L. R., Evans C. J., Davies B., Kudritzki R.-P., Gazak J. Z., Bergemann M., Plez B., Ferguson A. M. N., 2015, ApJ, 803, 14

Rayleigh L., 1880, MNRAS, 40, 254

Sharples R., 2015, in IAU Symposium, Vol. 309, Galaxies in 3D across the Universe, Ziegler B. L., Combes F., Dannerbauer H., Verdugo M., eds., pp. 11–16

Sharples R. et al., 2006, , 50, 370

Tubbs E. F., Goss W. C., Cohen J. G., 1982, in Society of Photo-Optical Instrumentation Engineers (SPIE) Conference Series, Vol. 331, Instrumentation in Astronomy IV, p. 289

Young T., 1802, Phil. Trans. R. Soc. Lond., 92, 12